THE JOURNAL OF PHYSICAL CHEMISTRY C

Article

pubs.acs.org/JPCC

Nitrogen Adsorption, Dissociation, and Subsurface Diffusion on the Vanadium (110) Surface: A DFT Study for the Nitrogen-Selective Catalytic Membrane Application

Panithita Rochana, Kyoungjin Lee, and Jennifer Wilcox*

Department of Energy Resources Engineering, Stanford University, 367 Panama Street, Room 65, Stanford, California 94305, United States

Supporting Information

ABSTRACT: Catalytic nitrogen (N_2)-selective membrane technology with potential applications of indirect CO_2 capture and ammonia synthesis is introduced. Metallic membranes made from Earth-abundant group V metals, i.e., vanadium (V), and alloys with ruthenium (Ru) are considered. Similar to a traditional palladium (Pd)-based hydrogen (H_2)-selective membrane for hydrogen purification, N_2 molecules preferentially adsorb on the catalytic membrane and dissociate into two nitrogen atoms. Atomic nitrogen subsequently diffuses through the crystal lattice by hopping through the interstitial crystal sites of the bulk metal, ultimately leading to atomic nitrogen on the permeate side of the membrane. This study is focused on the nitrogen interactions only at the membrane surface and the first subsurface layer. The adsorption energies of molecular as well as atomic nitrogen on the vanadium surface (V(110)) and Ru-alloyed V surface (V_xRu_{100-x}/V(110), where x is the atomic composition of vanadium in the alloy) are calculated using first-principles and compared against traditional catalysts for ammonia synthesis, i.e., iron (Fe). The N_2 dissociation pathway and its corresponding activation barrier are also determined. Additionally, the diffusion of atomic nitrogen from the V(110) surface to its subsurface layers is investigated to determine the rate-limiting step of nitrogen transportation across membrane surface. It has been found that N_2 and atomic nitrogen bind on the V(110) surface very strongly compared to adsorption on corresponding Fe surfaces. Although the activation energy (ca. 0.4 eV) for nitrogen dissociation on the V(110) surface is greater than that of the Fe surfaces, it is comparable to that of the Ru surfaces. Atomic nitrogen slightly prefers to stay on the V(110) surface rather than in the subsurface layers. Coupling this with the relatively high activation barrier for subsurface diffusion (ca. 1.4 eV), it is likely that the subsurface diffusion of nitrogen is the rate-limiting step of nitrogen transport across a membrane. Alloying Ru with V reduces the adsorption energy of atomic nitrogen on the Ru-alloyed V(110) surface in addition to the subsurface layer. Therefore, it is expected to facilitate nitrogen transport across the membrane surface.

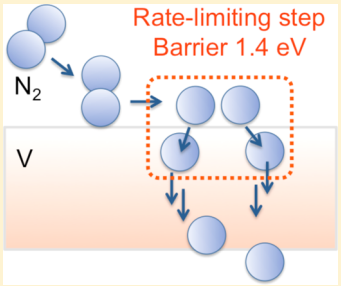

1. INTRODUCTION

Metallic membranes made from Earth-abundant group V metals, i.e., vanadium (V), are considered for catalytic selective N_2 separation with the potential benefit of ammonia synthesis with indirect CO_2 capture. This N_2-selective membrane technology benefits from the driving force of N_2 in flue gas (73 wt %) streams for indirect CO_2 capture as it can possibly create a sufficient external driving force, i.e., partial pressure across a membrane. The concept of a N_2-selective membrane stems from the development of H_2-selective metallic membranes for H_2 purification processes. The application of the H_2-selective metallic membranes significantly draws a great deal of attraction because they are commercially available and may be fabricated into large-scale continuous films.[1] Figure 1 proposes the schematic of a N_2-selective membrane reactor for postcombustion capture applications. N_2 molecules preferentially adsorb on the catalytic membrane and dissociate into two nitrogen atoms. The atomic nitrogen then diffuses through the crystal lattice by hopping through the interstitial crystal sites of the bulk metal, ultimately leading to atomic nitrogen on the permeate (or sweep) side of the membrane. The flux of N_2 across the membrane is dependent upon a partial pressure driving force, which can be created by using H_2 as a sweep gas. The use of H_2 as a sweep gas may allow for the synthesis of ammonia and CO_2 would be effectively separated on the high-pressure retentate side of the membrane for further use.

The use of a catalytic membrane to change the architecture of a traditional catalytic reactor allows the use of strong-binding transition metals on the far left of the periodic table, such as Earth-abundant group V metals, i.e., vanadium (V), niobium (Nb), and tantalum (Ta) for ammonia synthesis. These transition metals are known to bind adsorbates too strongly, leading to poor turnover rates. However, these metals are known to be very permeable to H_2.[2−4] The H_2 permeability at 500 °C is 1.6×10^{-6} mol/(m s $Pa^{1/2}$) for Nb, 1.3×10^{-7} mol/(m s $Pa^{1/2}$) for Ta, and 1.9×10^{-6} mol/(m s $Pa^{1/2}$) for V.[5] Therefore, it is interesting to study how well nitrogen would interact on these metals. Among the three transition metals of

Received: November 30, 2013
Revised: February 7, 2014
Published: February 7, 2014

dx.doi.org/10.1021/jp411763k | J. Phys. Chem. C 2014, 118, 4238−4249

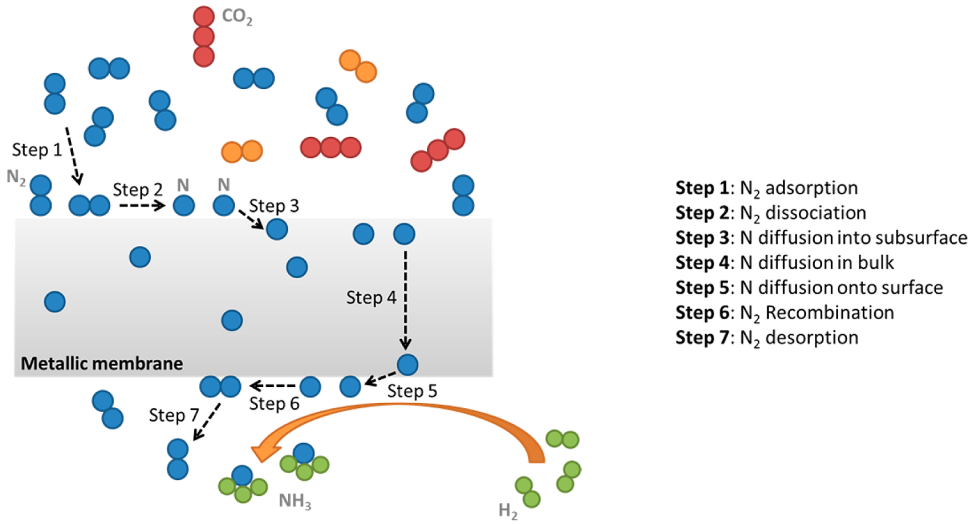

Figure 1. Schematic of catalytic N_2-selective metallic membrane with ammonia synthesis.

the group V elements, vanadium is chosen in this study due to its great abundance in the Earth's crust, resulting in potentially low fabrication costs.[6]

To the authors' knowledge, there are limited literature studies focusing on the interaction of molecules on the V surface since the preparation of the clean V surface is rather difficult and time-consuming.[7−13] In addition, there are no previous studies to reflect upon due to the novelty of this N_2-selective membrane technology. Consequently, the nitrogen interaction on the V surface is of central interest to the current study. Fundamental investigation of N_2 and atomic nitrogen adsorption, dissociation, and potential subsequent atomic diffusion on and within V are examined from first-principles. The adsorption energies of N_2 as well as atomic nitrogen on the V surface (V(110)) and Ru-alloyed V surface (V_xRu_{100-x}/V(110), where x is the atomic composition of vanadium in an alloy) are calculated and compared against traditional catalysts used for ammonia synthesis, i.e., iron (Fe). The N_2 dissociation pathway and its corresponding activation barrier are also determined via the climbing image nudged elastic band (CI-NEB) method. Additionally, the diffusion of atomic nitrogen from the V(110) surface to its subsurface layers is investigated to determine the rate-limiting step of nitrogen transport across the membrane surface.

To determine the feasibility of using V as a material for a N_2-selective membrane, the barrier for N_2 dissociation on the V(110) surface is compared with the barriers on the Fe and Ru surfaces as they are well-studied for ammonia synthesis. In addition, the first subsurface diffusion barrier of atomic nitrogen into the subsurface of V is compared with the well-studied H/Pd case since Pd-metallic membranes are commercially available for H_2 purification from natural gas reforming processes.

This study is organized as follows: in section 2, the computational details and the system are presented; in section 3 the results of nitrogen interactions with the vanadium surface are discussed; and in section 4, a conclusion of the current study and the future research directions is provided.

2. COMPUTATIONAL METHODOLOGY

All calculations are based on plane-wave density functional theory (DFT) and performed using the Vienna *ab initio* simulation package (VASP).[14,15] The electron−ion interactions are represented by the projector-augmented wave (PAW) approach,[16,17] and the electron exchange correlation effects are described by a generalized-gradient approximation (GGA) using the Perdew−Burke−Ernzerhof functional[18] with a plane-wave expansion with a cutoff of 600 eV. The surface Brillouin zone integration is calculated using a Monkhorst−Pack mesh.[19] During geometry optimization, the conjugate-gradient (CG) algorithm is applied to relax the ions into their instantaneous ground state, and electron smearing with a width of 0.05 eV is employed via the first-order Methfessel−Paxton technique[20] for improved convergence. Geometry convergence is achieved when the forces on all unconstrained atoms are less than 0.02 eV/Å.

The climbing image nudged elastic band (CI-NEB) method developed by Jónsson and co-workers[21] is used to determine the minimum energy paths (MEPs) and corresponding transition states for N_2 dissociation on the vanadium surface as well as subsurface diffusion of atomic nitrogen into the V surface. Once the initial and final configurations of a process are known, an interpolated chain of configurations (images) between the initial and the final states is created. The intermediate configurations (images) are connected by springs and relaxed simultaneously to the MEP, through which the highest-energy configuration climbs uphill to the saddle point.[21] A 5 eV/Å^2 spring constant is used in all CI-NEB calculations. The nature of the transition state found by the CI-NEB method is determined by diagonalizing a finite difference construction of the Hessian matrix with displacements of 0.015 Å. Only nitrogen atoms are allowed to move, while V atoms are kept fixed at their relaxed geometries.

Metallic vanadium has a body-centered cubic (bcc) structure with an experimental lattice constant of 3.024 Å.[22] The theoretical lattice constant found in this study is 2.98 Å, which compares well against the experimental value. To optimize the computational cost and the accuracy of the DFT calculations, a seven-layer slab of the V(110) surface with a single-sided vacuum region of 15 Å is simulated as three-dimensional infinite periodic structures by defining a supercell and periodic boundary conditions in all three principal axes. Two surface models, i.e., (1 × 1) and (2 × 2) structures as shown in Figure

dx.doi.org/10.1021/jp411763k | J. Phys. Chem. C 2014, 118, 4238−4249

2, are used in this study with a corresponding k-mesh[19] of 14 × 14 × 1 and 7 × 7 × 1, respectively.

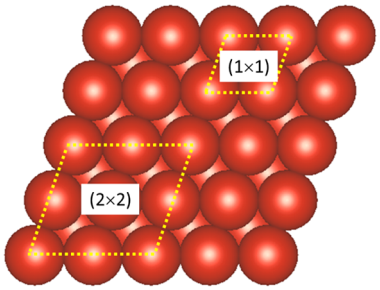

Figure 2. Top view of the V(110) surface with yellow line indicating the (1 × 1) and (2 × 2) surfaces.

The adsorbate, i.e., N_2 or atomic nitrogen, is placed on one side of the V(110) surface, thereby producing a dipole moment due to the surface charge rearrangement. However, a dipole moment correction is not included in this study since it has a negligible effect on the total energy (i.e., <0.01 eV/cell) in both the clean V(110) surface and N_2-adsorbed surface systems. During the geometry optimization of the adsorbed system, the bottom four layers of the V(110) surface are kept frozen at the estimated bulk parameters, while the top three layers of the V(110) surface and the adsorbate, i.e., nitrogen molecules or atoms, are allowed to relax to their optimized geometries.

The ad(b)sorption energy of nitrogen on (in) the V(110) surface can be calculated with respect to either the isolated N_2 molecule (eV/N_2) or isolated nitrogen atom (eV/N) as shown in eqs 1 and 2, respectively.

$$E_{ads}\ (\mathrm{eV/N_2}) = \frac{1}{n}[E(\mathrm{V(110) + N_2}) - E(\mathrm{V(110)}) - nE(\mathrm{N_2})] \quad (1)$$

$$E_{ads}\ (\mathrm{eV/N}) = \frac{1}{n}\left[E(\mathrm{V(110) + N}) - E(\mathrm{V(110)}) - \frac{n}{2}E(\mathrm{N_2})\right] \quad (2)$$

where $E(\mathrm{V(110) + N_2})$ and $E(\mathrm{V110 + N})$ are the total free energies of the nitrogen-adsorbed systems. The term E(V-(110)) is the total free energy of the clean V(110) surface, n is number of nitrogen molecules or atom on the supercell, and $E(\mathrm{N_2})$ is the total free energy of the nitrogen molecule in the gas phase, which is calculated by placing the N_2 molecule in a 15 × 15 × 15 Å^3 cubic box and carrying out a Γ-point calculation. The calculated N_2 bond length is 1.113 Å with a vibrational frequency of 2421 cm^{-1}. These values are in reasonable agreement with experimental data of 1.098 Å and 2359 cm^{-1}, respectively.[22] A negative E_{ads} value indicates the stabilized adsorption of the nitrogen molecule or atom relative to the separated V(110) surface and adsorbate. The more negative adsorption energy implies a more preferable adsorption location on the surface.

3. RESULTS AND DISCUSSION

3.1. N_2 Adsorption on V(110) at 0.25 ML. Figure 3a illustrates the top view of the V(110) surface with labels for the available adsorption sites. There are four possible sites on the surface, i.e., top site, short-bridge site (SB), long-bridge site (LB), and the 3-fold hollow site (TF). Figure 3b shows a schematic of a side view of the V(110)-N_2 surface for the N_2 molecule at the top site, in which the tilting angle (θ) is indicated. Note that θ is the deviation from the surface normal. In this study two initial N_2 orientations are tested on the V(110) surface, including (1) the *perpendicular orientation*, or γ state, in which the molecular axis is along the surface normal direction, i.e., θ = 0°, and (2) the *parallel orientation*, or α state, in which the molecular axis is in-plane with the V(110) surface, i.e., θ = 90°. Since N_2 is allowed to relax during the geometry optimization, the adsorbed N_2 structure may be different from the initial N_2 structure after the calculation converges.

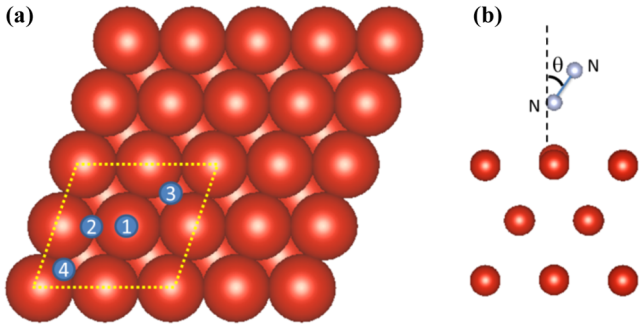

Figure 3. Schematic of (a) the top view with the following possible adsorption sites on the V(110) surface. 1: top; 2: short-bridge (SB); 3: long-bridge (LB); 4: 3-fold hollow (TF). (b) Side view of V(110)-N_2, in which θ is the tilting angle.

The most stable configurations of N_2 adsorption on the V(110) surface at 0.25 ML surface coverage and their corresponding adsorption energies are tabulated in Table 1. It is crucial to determine the nature of the adsorbed states, i.e., whether it is the true adsorption state (local minima), the transition state (first-order saddle point), or the higher-order saddle point by carrying out a frequency analysis. If the frequencies of a particular optimized geometry are real numbers, then the structure is the minimum or the true adsorption state. The transition states are identified as having one imaginary frequency, while the higher-order saddle points have more than one imaginary frequency. The real number frequencies in Table 1 indicate that the stable adsorbed states are all in local minima. The corresponding optimized structures of the local minima at the stable adsorbed states are illustrated in Figure 4. Molecular N_2 generally prefers to adsorb at high metal coordination sites and molecular N_2 binds strongest on the LB site in a parallel orientation, with a corresponding adsorption energy of −2.82 eV/N_2. The second strongest adsorption site is the SB site with an adsorption energy of

Table 1. Adsorption Energies of Stable Adsorbed Molecular N_2 on the V(110) at 0.25 ML Surface Coverage and Their Structural Parameters

				vibration frequency (cm^{-1})	
	E_{ads} (eV/N_2)	d(N–N) (Å)	h(N–surf) (Å)	N–N stretching	N–metal stretching
α state (LB)	−2.82	1.305	1.268	1222.26	457.29
α' state (SB)	−2.27	1.334	1.297	1086.84	446.47
γ state (top)	−0.54	1.134	2.025	2155.32	286.91

dx.doi.org/10.1021/jp411763k | J. Phys. Chem. C 2014, 118, 4238−4249

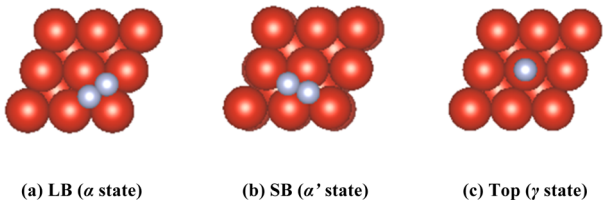

Figure 4. Optimized structures of molecular N_2 adsorption at 0.25 ML surface coverage on (a) LB (α state), (b) SB (α' state), and (c) top (γ state) sites.

−2.27 eV/N_2 with the adsorbed N_2 molecule lying parallel on the surface. In addition, slight surface reconstruction after adsorption is observed at this site. The adsorption on LB and SB sites in a parallel orientation is labeled as α and α' state in this study. Of the three local minima, the N_2 molecule adsorbed in the upright position at the top site has the weakest adsorption energy of −0.54 eV/N_2. This is labeled as γ state in this study. The adsorption strength of molecular N_2 onto the surface varies in the order $\alpha > \gamma$. However, this is not always the case if the N_2 molecule adsorbs at high coverage on the metal surface in which case the γ state becomes more stable than the α state.[23,24] The N−N bond length, d(N−N), of the optimized geometries is in the range of 1.134−1.334 Å. Clearly, the N−N bond length increases upon N_2 adsorption to the surface compared to the calculated N−N bond length in the gas phase (1.113 Å). Moreover, the N−N stretching frequencies decrease from 2421 cm^{-1} in the gas phase to ∼1223, 1087, and 2156 cm^{-1} for α-, α'-, and γ-N_2, respectively. In high-resolution electron energy loss spectroscopy (HREELS) measurements, the N−N stretching frequency for the α state occurs in the range of 1150−1600 cm^{-1}, with the 2100−2250 cm^{-1} region indicative of the γ state.[23] An increase in the N−N bond length and decrease in the N−N stretching frequency is evident from the weakening N−N interaction of the N_2 molecule and the subsequent tendency for dissociation. Therefore, the α and α' states are regarded as a precursor state for N_2 dissociation on V(110) as they are on other metal surfaces.[23] The entire calculation results including less stable configurations are shown in Table S1 of the Supporting Information.

Literature values for the N_2 adsorption energies on Fe[23−27] and Ru[28,29] surfaces are tabulated in Table 2. The (111) plane of Fe is selected for comparison because it is the most reactive surface toward N_2 adsorption[26] and ammonia synthesis.[30−34] In the case of the Ru surface, the (0001) plane is the most close-packed structure for this metal. Therefore, several detailed experiments and theoretical calculations have been performed on this surface. An additional δ state is observed both experimentally and theoretically on the Fe and Ru surfaces. This state is associated with molecular N_2 adsorption in a perpendicular orientation and is less stable than the γ state. The δ state is only populated when the surface is saturated with the γ state. A comparison of the N_2 adsorption energies at 0.25 ML surface coverage in Table 2 reveals that the adsorption energy of the γ-N_2/V(110) structure falls within the adsorption energy range of γ-N_2 on Fe and Ru surfaces. However, the α- and α'-N_2 states bind to the V(110) surface considerably stronger than those on the Fe surfaces. Weak interactions occur in γ state mainly due to the overlapping of the $3\sigma_g$ bonding orbital of a nitrogen molecule with the bands of metal surface. On the other hand, α state interactions are achieved through the donation from $1\pi_u$ bonding orbital to the surface and subsequent back-donation from the surface to the $1\pi_g$* orbital. If the interaction through the π-orbitals becomes more compelling, e.g., in the case of V(110) surface, nitrogen−metal interaction becomes stronger while nitrogen−nitrogen bond is substantially weakened. This may lead to dissociation as we expect from the bond length and frequency analysis. It is reported in other studies that dissociative adsorption is favored for nitrogen adsorption on V surfaces.[35] A strong interaction particularly on V(110) may be described using the d-band center model, which was developed by Hammer and Nørskov.[36] The d-band model explains the trend in chemisorption energies on different transition metals. As an adsorbate binds to a transition metal the formation of bonding and antibonding states occurs below and above the metal d bands. If the antibonding states for the adsorbate are filled, the bonding between the adsorbate and the transition metal becomes weak. The occupancy of the antibonding state is determined by not only the extent of filling of the d states but also the position of the antibonding states relative to the Fermi level. The Fermi level in metals is defined by the energy of the highest occupied states at a temperature of absolute zero. As the d band shifts up in energy, the number of antibonding states above the Fermi level increases, leading to less-filled antibonding states and a subsequently stronger bond. For the same transition metal series, e.g., 3d, 4d, or 5d series, the number of d electrons decreases and the d band shifts up in energy toward the Fermi level from right to left in the periodic table.[37] Consequently, the N_2 adsorption energy is expected to be stronger on vanadium, which is an early transition metal.

3.2. Atomic Nitrogen Adsorption on V(110). At 0.25 ML coverage, two local minima are observed as indicated in Table 3. The optimized structures associated with these two

Table 2. Literature Values for Adsorption Energies of Molecular N_2 on Different Transition Metal Surfaces

	E_{ads} (eV/N_2)		
	γ state	α state	δ state
polycrystalline Fe films[23]	ca. −0.23 (exp)	ca. −0.44 (exp)	ca. −0.20 (exp)
Fe(111), 1/3 ML	−0.3 (exp)[25]	−0.41 (exp)[26,27]	−0.21 (calc[a])[24]
	−0.35 (calc[a])[24]	α, −0.41 (calc[a])[24]	
		α', −0.17 (calc[a])[24]	
Fe(111), 1 ML[24]	−0.34 (calc[a])	α, −0.15 (calc[a])	N/A
		α', −0.01 (calc[a])	
Ru(0001), 1/3 ML	−0.44 (exp)[28]	N/A	−0.25 (exp)[29]
	−0.33 (exp)[29]		
	−0.61 (calc[a])[28]		

[a]Calculations in refs 24 and 28 were performed by DFT using an ultrasoft pseudo potential with PW91 exchange-correlation functional.

dx.doi.org/10.1021/jp411763k | J. Phys. Chem. C 2014, 118, 4238−4249

Table 3. Adsorption Energies of Atomic Nitrogen and the Structural Parameters, at 0.25 and 0.50 ML Surface Coverage

	E_{ads} (eV/N)	h(N−surf) (Å)	N−metal stretching (cm^{-1})
	0.25 ML surface coverage		
LB	−2.37	0.311	251.02
TF	−2.16	0.980	539.70
	0.50 ML surface coverage		
β state (LB−LB)	−2.34	0.256	296.71
β' state (LB−Top−LB)	−2.00	0.877	600.42
TF−TF	−1.53	1.004	600.23

local minima are shown in Figure 5. Entire calculation results including less stable states can be found in Table S2 of the

(a) LB (b) TF

Figure 5. Optimized structures of atomic nitrogen adsorption at 0.25 ML surface coverage on (a) LB and (b) TF sites.

Supporting Information. Similar to the stable adsorbed N_2 state, atomic nitrogen prefers to adsorb on high metal coordination sites, i.e., LB and TF sites. There is surface reconstruction of the V(110) plane upon atomic nitrogen adsorption at the LB site as seen in Figure 5a. The top layer of the V(110) surface slightly reconstructs into a V(100)-like structure, where atomic nitrogen is positioned at the 4-fold hollow site. Additional calculations of atomic nitrogen adsorption at the LB site on the unreconstructed V(110) surface have been performed. The calculated adsorption energy on the unreconstructed V(110) surface of atomic nitrogen is −2 eV/N, which is less stable than the adsorption on the reconstructed surface. This surface reconstruction only occurs upon nitrogen adsorption at the LB site.

At 0.5 ML coverage, three local minima have been determined and their optimized geometries are presented in Figure 6. The adsorption energies and the structural parameters

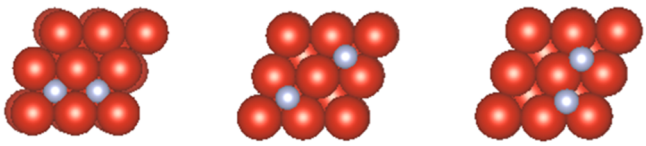

(a) LB-LB (β state) (b) LB-Top-LB (β' state) (c) TF-TF

Figure 6. Optimized structures of atomic nitrogen adsorption at 0.50 ML surface coverage at (a) LB−LB (β state), (b) LB−Top−LB (β' state), and (c) TF−TF sites.

are provided in Table 3, and the entire calculation results including less stable states can be found in Table S3 of the Supporting Information. The high coordination sites, i.e., LB and TF sites, remain the strongest adsorption sites for atomic nitrogen. Since chemisorbed nitrogen on transition metal surfaces is conventionally identified as the β state,[23] the two of the most stable states associated with the LB−LB and LB−Top−LB in this study are labeled as β and β' states, respectively. Only the β state induces the reconstruction of the V(110) surface as shown in Figure 6a. Similar to atomic nitrogen adsorption on the LB site with 0.25 ML coverage, the top layer of the V(110) surface reconstructs into a V(100)-like structure, where nitrogen atoms sit at the 4-fold hollow sites. However, the surface reconstruction upon 0.5 ML atomic nitrogen adsorption is more apparent than that at 0.25 ML coverage. Although one would expect weaker adsorption energy on the same adsorption site with higher surface coverage, atomic nitrogen at the LB−LB site (0.5 ML) binds as strongly as the nitrogen atom at the LB site (0.25 ML). This infers that the surface reconstruction indeed allows the atomic nitrogen adsorbed system to gain additional adsorption energy toward the more stable adsorption configuration. However, it has been found that the adsorption energies on the LB−Top−LB and the TF−TF sites are lower than those energies on the same sites with 0.25 ML coverage by 0.37 and 0.64 eV/N, respectively. The weaker adsorption energy may be due to the lateral interaction between neighboring nitrogen atoms and no reconstruction of the surface.

The N atom usually occupies the 4-fold hollow sites above the transition metal surfaces in general. For the adsorption of atomic nitrogen on Fe single crystal surfaces, temperature-programmed desorption (TPD) experimental results on Fe(110), (100), and (111) surfaces show that the adsorption energy ranges between −1.05 and −1.15 eV/N (equivalent to −2.1 and −2.3 eV/N_2).[26,38] Meanwhile, the adsorption energy changes from −1.1 to −0.25 eV/N (equivalent to −2.2 to −0.5 eV/N_2) over a surface coverage range from 0 to 0.7 ML across real catalysts for ammonia synthesis.[39] On the Fe(100) surface, nitrogen atoms form a very stable c(2 × 2) structure with a saturation coverage of 0.5 ML.[40] This overlayer structure is also found on the Fe(111) and (110) surfaces, while LEED results suggest that the surface reconstructs upon atomic nitrogen adsorption.[26,38] Mortensen et al.[41] performed the DFT calculation using ultrasoft pseudopotential with PW91 exchange-correlation functional to determine the adsorption energies and structures for nitrogen atoms on three Fe surfaces including (110), (100), and (111). They found that the adsorption energies on the unreconstructed Fe(111) and (110) surfaces are much smaller than those on the Fe(100) surface because of the lack of 4-fold symmetry that is only present on the Fe(100) surface.[41] Therefore, islands of a c(2 × 2)-N/Fe(100)-like layer are suggested to appear on the Fe(111) and (100) surfaces after atomic nitrogen adsorption in order to obtain increased adsorption energy.[24,41] On the Ru(0001) surface, atomic nitrogen also favors the high coordination sites. The adsorption energies are found to be −0.77 eV/N for p(2 × 2)-N/Ru (0.25 ML) and −0.19 eV/N for c(2 × 2)-N/Ru (0.5 ML). No surface reconstruction from nitrogen adsorption has been reported in the literature. As seen in Tables 3, the atomic adsorption energies at the most stable site on the V(110) surface are considerably stronger than those on the Fe and Ru surfaces. The reason for such strong adsorption of atomic nitrogen on the V(110) surface is similar to the case of the adsorbed α-N_2 adsorption that may be explained by d-band theory.

3.3. N_2 Dissociation Pathway on V(110). The N_2 dissociation on the Fe(111) surface[24] is known to follow a complicated dissociation path: $\gamma \rightarrow \delta \rightarrow \alpha \rightarrow \alpha' \rightarrow \beta$. Since both V and Fe have a bcc crystal structure, the N_2 dissociation on the V(110) surface is proposed to be potentially analogous

dx.doi.org/10.1021/jp411763k | J. Phys. Chem. C 2014, 118, 4238−4249

to its dissociation on the Fe surface selected. The N_2 molecules are initially trapped into a highly mobile γ state for the removal of excessive energy. This γ state appears to be the precursor state for the α state as the N_2 molecule in the γ state tilts to a parallel bound α state at an appropriate hollow site.[42,43] An additional α state, i.e., α' state, is found only from the theoretical calculation since it is less stable than the other stable adsorbed states and is subsequently difficult to be observed experimentally. This α' state is more likely the precursor state to N_2 dissociation than the α state as it has a longer nitrogen bond and a smaller N−N stretching vibrational frequency indicating a weaker N−N bond upon adsorption.[24]

There are many possibilities for the MEP associated with N_2 dissociation on the V(110) surface. To gain a deeper understanding of the N_2 dissociation process on the V(110) surface, 2D slices in the potential energy surface of N_2 dissociation for different paths are constructed by a series of single-point energy calculations of dissociated nitrogen atoms. The optimized clean V(110) surface is used and kept fixed for all dissociation paths considered. Dissociated nitrogen atoms are placed on the fixed V(110) surface and the calculations are performed at several heights (h) above the surface and N−N bond lengths (r) along the dissociation paths. Within the potential energy surface (PES) construction, h is varied from 0.5 to 2.4 Å and r is changed from 1.1 to 4.6 Å along the reaction coordinates. At least 120 calculations are carried out for each N_2 dissociation path by varying the height and the N−N bond length within the provided ranges. Three dissociation paths are investigated within the 2D PES: (1) molecular N_2 at the α' state to atomic nitrogen at the β state; (2) molecular N_2 at the α state to atomic nitrogen at the β' state via the *short* diagonal of the unit cell; and (3) molecular N_2 at the α state to atomic nitrogen at the β' state via the *long* diagonal of the unit cell. Dissociation from the α state to the β state is not included in this study because it shows a higher barrier than for the dissociation path via the α' state and therefore is likely not to be a dominant pathway.

The PES for N_2 dissociation on the V(110) surface is presented in Figures 7 and 8. The initial state, final state, and proposed transition state (TS) are all located on the PES diagram. It is important to note that the dissociation barriers obtained from the PES do not reflect the actual barrier for N_2 dissociation on the V(110) surface. However, this information provides a starting point for the prediction of the MEP for dissociation. Comparing the three dissociation paths, the dissociation from α'-N_2 to β-N has the lowest barrier. On the other hand, the dissociation from α-N_2 to β'-N via either short or long diagonal configurations has to overcome a larger barrier because the nitrogen atom has to move around the V atom that is coordinated to the second nitrogen atom. Consequently, the MEP for N_2 dissociation on the V(110) surface is expected to occur via the dissociation from α'-N_2 to β-N, and the following N_2 dissociation path on the V(110) surface is proposed: γ-N_2 → α'-N_2 → β-N. According to the CI-NEB calculation, Figure 9 presents the MEP for the proposed dissociation on the V(110) surface. The N_2 transition from the γ to the α' state is found to be nonactivated on the V(110) surface as the energy of the N_2 molecule decreases along the reaction path. Conversely, the N_2 transition from the α' state to the dissociated β state is an activated process. The corresponding dissociation barrier is 0.4 eV, and the transition state structure is shown in Figure 9.

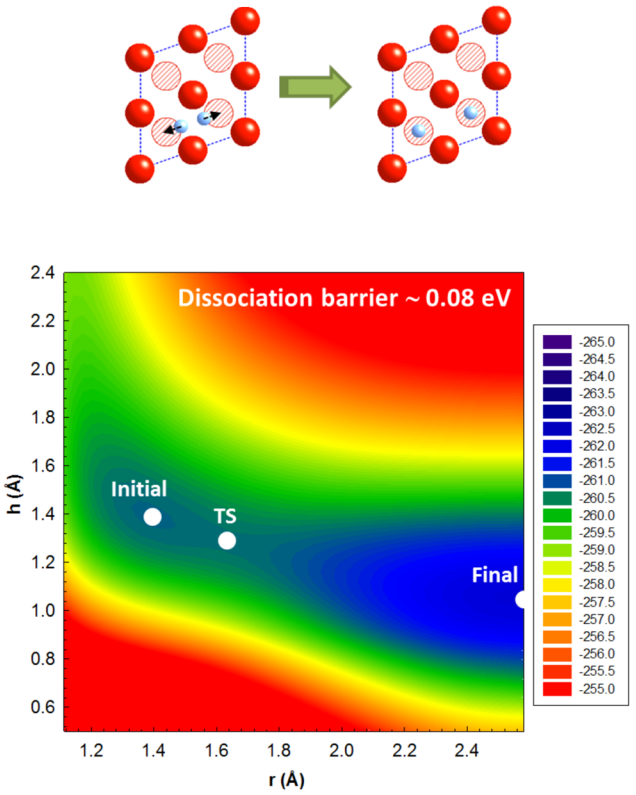

Figure 7. Potential energy surface along the 2D reaction path for N_2 dissociation from α'-N_2 to β-N; energy units are given in eV.

The calculated dissociation barrier for N_2 dissociation on the V(110) surface is then compared against the N_2 dissociation barriers on Fe and Ru surfaces. The dissociation of N_2 on the Fe(111) surface has no barrier.[24] On the other hand, the barrier for dissociation on the V(110) surface is comparable to that on the Ru(0001)-step surface, i.e., 0.4 eV.[44−46] Since Ru is also a traditional catalyst for ammonia synthesis, which also involves N_2 dissociation, it is reasonable to conclude that the V(110) surface may be an active surface for N_2 dissociation. However, following dissociation, the dissociated state binds to the V(110) surface considerably stronger than it does to the Fe(111) and the Ru(0001) surfaces. This strong adsorption energy may play an important role in the subsurface diffusion of atomic nitrogen into the V(110) surface.

3.4. Atomic Nitrogen Diffusion into Subsurface Layer of V(110). Typical interstitial sites for atomic nitrogen in the subsurface are illustrated in Figures 10a and 10b. These are the octahedral (O-) and the tetrahedral (T-) sites of the crystal lattice, represented by a black dot. For atomic nitrogen in the subsurface, the nitrogen atom prefers the high coordination site, i.e., the O-site just as in bulk vanadium.[47] The optimized geometry for nitrogen absorption is presented in Figure 10c. The calculated absorption energy of the nitrogen atom in the first subsurface O-site is −2.29 eV/N. This absorption energy is slightly less stable than the adsorption energy of atomic nitrogen on the surface at the LB site (−2.37 eV/N). This indicates that the nitrogen atom somewhat favors an adsorbed state on the V(110) surface rather than an absorbed state in the subsurface layer. The atomic nitrogen absorption at the first subsurface T-site, on the other hand, is not stable. The nitrogen atom moves either to the surface or to the first subsurface O-site after geometry optimization. A distortion in the host

dx.doi.org/10.1021/jp411763k | J. Phys. Chem. C 2014, 118, 4238−4249

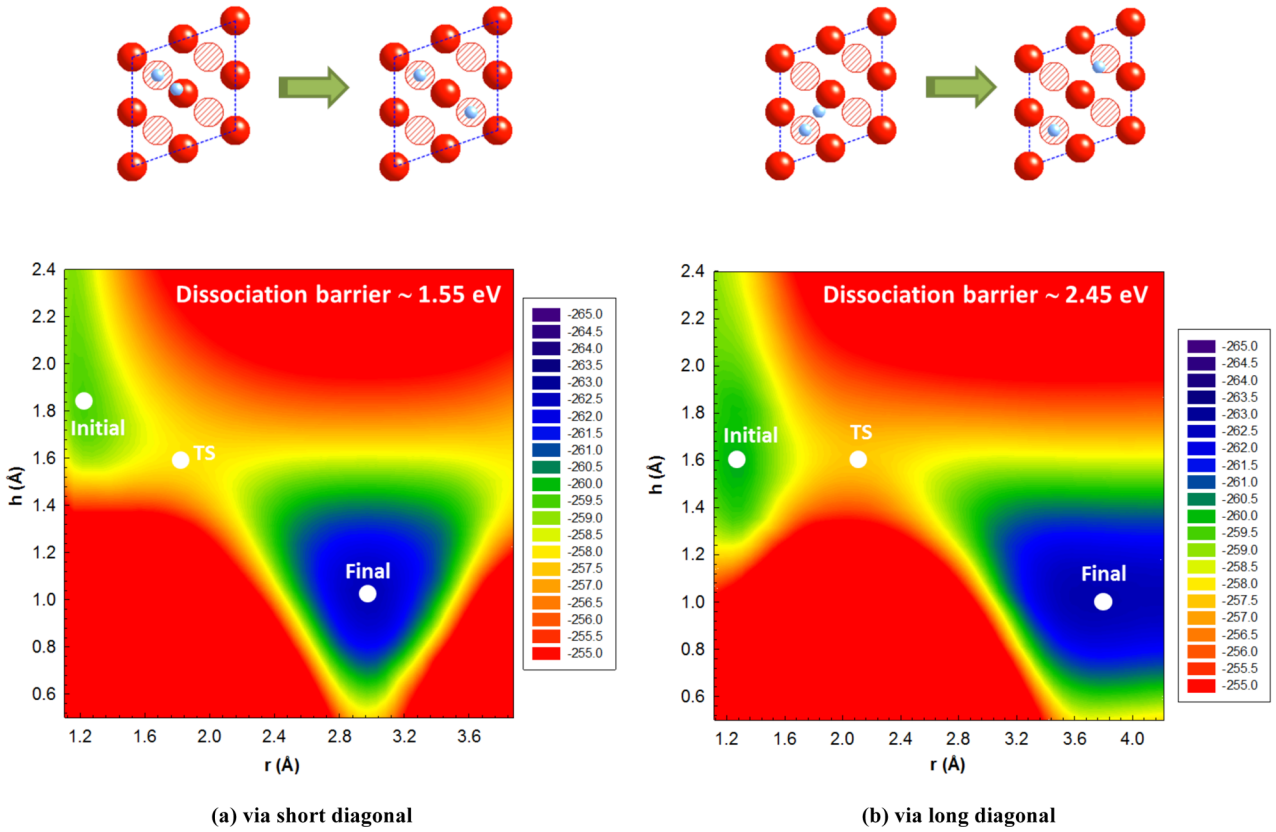

(a) via short diagonal (b) via long diagonal

Figure 8. Potential energy surface along the 2D reaction paths for N_2 dissociation: (a) α-N_2 to β'-N via the *short* diagonal and (b) α-N_2 to β'-N via the *long* diagonal configurations.

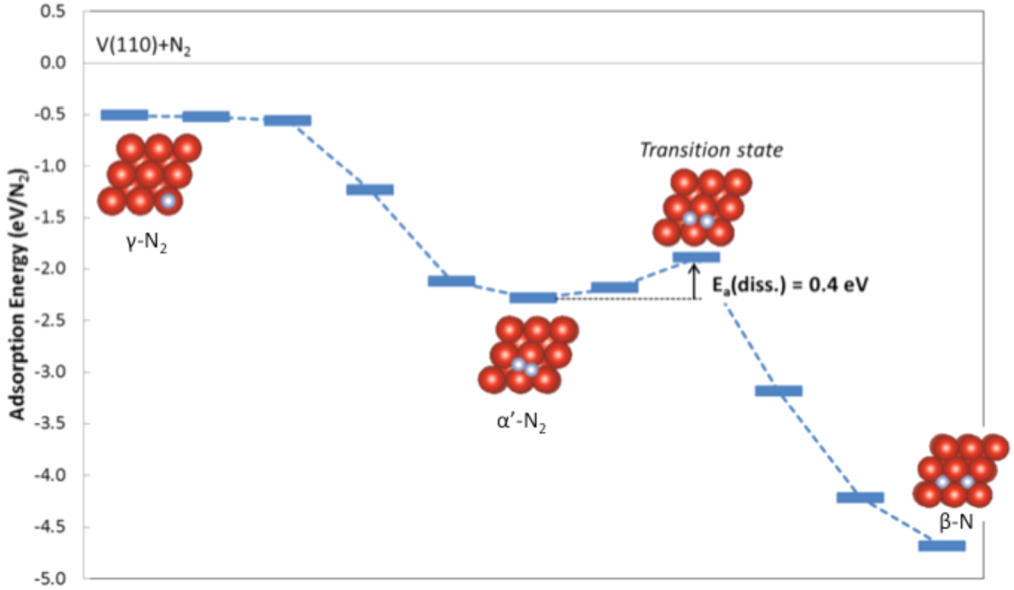

Figure 9. Proposed minimum-energy path for N_2 dissociation on the V(110) surface.

V(110) structure upon the presence of the nitrogen atom in the interstitial sites is shown in Figure 10c. The surface V atom that is coordinated to atomic nitrogen is pushed toward the vacuum region by 0.47 Å. This same phenomenon is also found from theoretical studies on carbon dissolution and diffusion in bulk Fe[48] and carbon absorption in the subsurface of Fe(110),[49] in which one surface Fe atom is pushed toward the vacuum region by 0.5 Å. Such distortion occurs in order to reduce the strain caused by the interstitial atom, which is atomic nitrogen in this case.

Table 4 provides the existing information from selected well-known systems. The carbon and hydrogen diffusion in iron is chosen because it represents a system in which interstitial diffusion may cause problems including strain aging, embrittlement, and steel erosion.[48,49] On the other hand, hydrogen absorption and diffusion in metals such as palladium and

dx.doi.org/10.1021/jp411763k | J. Phys. Chem. C 2014, 118, 4238−4249

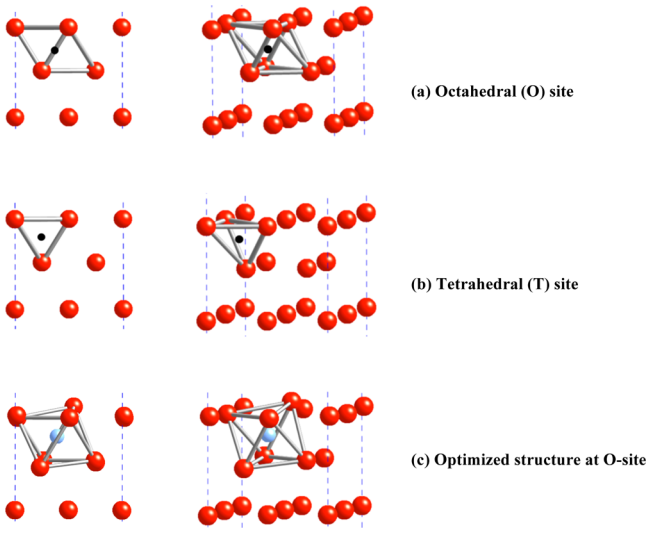

Figure 10. Possible interstitial sites for atomic nitrogen absorption in the subsurface of the V(110) surface at (a) octahedral (O-) site, (b) tetrahedral (T-) site, and (c) optimized structure at the O-site. The black dot in (a) and (b) represents the location of the interstitial site.

Table 4. Adsorption Energies on the Surface and Absorption Energies at the First Subsurface Layer of Selected Systems[a]

	E_{ads} (surface) (eV/atom)	E_{abs} (subsurface) (eV/atom)	reference
N/V(110)	−2.37	−2.29	this study
N/Fe(110)	−1.29	N/A	53
N/Fe(100)	−1.49	0.21	53
C/Fe(110)	−7.77	−7.30	49
C/Fe(100)	−8.24	−6.76	49
H/Fe(110)	−3.00	N/A	54
	−3.01	−2.03	51
H/Fe(100)	−2.65	−2.30	51
H/V(110)	−3.31	−2.40	51
H/V(100)	−2.97	−2.43	51
H/Pd(111)	−2.88	−2.58	51
H/Pd(110)	−2.81	−2.50	51

[a]The atomic coverage in all cases is equivalent to 0.25 ML.

vanadium are beneficial for hydrogen separation and purification processes.[50−52] According to Table 4, the interstitial atom prefers to stay on the surface compared to residing in the subsurface layer in every selected system. The adsorption energies of atomic nitrogen on the V(110) surface and in the first subsurface layer are in the same order of magnitude as those of the H/V and H/Pd systems. They are quite weak compared to the adsorption energies associated with the C/Fe system but slightly stronger than the N/Fe system. While the relative difference between the adsorption energy on the surface and in the subsurface provides insight that subsurface diffusion should be an activated process to overcome the unfavorable thermodynamic driving force, this does not indicate how fast the diffusion occurs.

The CI-NEB approach is applied to determine the possible MEP for nitrogen diffusion. Figure 11 shows the converged energy path for nitrogen diffusion into the V(110) surface at 0.25 ML surface coverage. The energy change from atomic nitrogen on the surface to the atomic nitrogen in the first subsurface layer is slightly endothermic. The corresponding subsurface diffusion barrier is 1.39 eV, while the reverse process has a barrier of 1.31 eV. At the transition state, the nitrogen atom stays approximately in the T-site, which neighbors three surface V atoms and one V atom in the subsurface layer.

In general, atomic diffusion through a metal is known to be the rate-limiting step for the transport through a metallic membrane. The literature values associated with diffusion usually refer to the barrier for bulk diffusion rather than subsurface diffusion, which may not be always true. Table 5 lists the subsurface diffusion barrier from the surface to the first subsurface layer of selected systems compared to the bulk diffusion barriers. The nitrogen diffusion in bulk vanadium was calculated, but it is not the focus in this study. The calculation details can be found in the Supporting Information. In Table 5, it is shown that the interstitial atom diffusion in the given bcc metals have a higher barrier for the first subsurface diffusion than the bulk diffusion. Therefore, the first subsurface diffusion can be assumed to be a rate-limiting step for atomic transport through metals.

Additional information regarding the feasibility of using vanadium as a material for a N_2-selective membrane can be gained by comparing the diffusion barriers of the N/V system with the well-studied H/Pd system since Pd and its alloys have long been used as metallic membranes for H_2 purification.[50,55] The barrier associated with subsurface diffusion from the H/Pd system is then used as a target for the proposed N_2-selective membrane concept. From Table 4, atomic hydrogen in the first subsurface layer is much less stable than atomic hydrogen on the surface. The diffusion barrier for hydrogen diffusion from the surface into the first subsurface layer is mostly due to the difference in the thermodynamic stability of these two states.[51] However, this is dissimilar for the N/V(110) case. The subsurface diffusion barrier for the N/V(110) surface is in the same order of magnitude as the barrier for the N/Fe or C/Fe system. This may be because nitrogen or carbon diffusion is more constrained with an associated higher barrier due to the large size of the atom compared to a hydrogen atom. In the case of carbon diffusion in iron, it has been found that the carbon atom prefers to stay on the surface rather than reside in the subsurface or the bulk.[49] Consequently, it is possible that the nitrogen atom is likely to stay on the V(110) surface since it also has a large barrier for subsurface diffusion, which is an undesirable property for a N_2-selective membrane. To engineer a more appropriate material for a N_2-selective membrane, one possible way is to weaken the adsorption energy through altering the surface of vanadium by alloying with other transition metals.

3.5. Preliminary Study of the Effect of Alloying V(110) with Ruthenium on Nitrogen Adsorption and Absorption. Ru is chosen as an alloy element for the V(110) surface because it is known to be an ideal catalyst for ammonia synthesis.[56] Since the expected operating temperature of the N_2-selective membrane is in the range of 500−800 °C, the Ru composition in the V−Ru alloy must not be greater than 25 atomic % in order to maintain the bcc crystal structure of the alloy according to the phase diagram of V−Ru alloy.[57] Consequently, one surface V atom is replaced by an atomic Ru atom as illustrated in Figure 12. This alloy surface is designated as $V_{75}Ru_{25}$/V(110).

The possible adsorption sites for thenitrogenatom on the $V_{75}Ru_{25}$/V(110) surface are shown in Figure 12. Four additional sites on the alloy surface have been investigated since the top layer is currently the alloy between V and Ru. The entire calculation results can be found in Table S4 of the

dx.doi.org/10.1021/jp411763k | J. Phys. Chem. C 2014, 118, 4238−4249

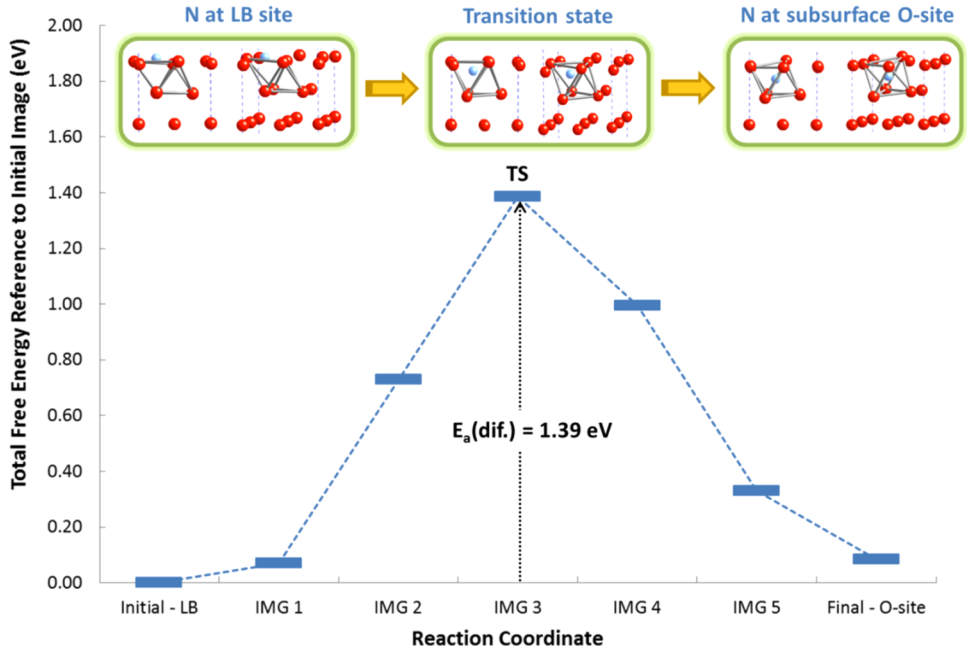

Figure 11. Proposed minimum-energy pathway for nitrogen diffusion into the first subsurface layer of the V(110) surface.

Table 5. Subsurface Diffusion Barrier (eV) from the Surface to the First Subsurface Layer of Selected Systems[a]

	E_a (eV)	barrier for bulk diffusion (eV)	reference
N/V(110)	1.39	1.10	this study (calc)
N/Fe(110) (0.11 ML)	1.50	0.72 (calc)	53
N/Fe(100) (0.25 ML)	1.80		53
C/Fe(110) (0.11 ML)	1.18	0.86 (calc)	48, 49
C/Fe(100) (0.11 ML)	1.47		48, 49
H/Fe(110)	0.99	0.05 (exp)	51
H/Fe(100)	0.36		51
H/V(110)	0.95	0.11 (exp)	51
H/V(100)	0.59		51
H/Pd(111)	0.40	0.23 (exp)	51
H/Pd(110)	0.41		51

[a]All calculations are performed at 0.25 ML coverage, unless noted otherwise.

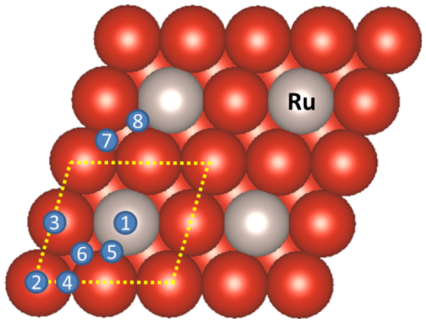

Figure 12. Schematic of the top view of the $V_{75}Ru_{25}$/V(110) surface with possible adsorption sites. 1: top Ru; 2: top V; 3: top V/next to Ru; 4: short-bridge V−V (SB-VV); 5: short-bridge V−Ru (SB-VRu); 6: long-bridge (LB); 7: 3-fold hollow V (TF-V); 8: 3-fold Ru (TF-Ru). Color legend: red = vanadium (V); gray = ruthenium (Ru).

Supporting Information. The high coordination site (i.e., LB) is the only stable site for atomic nitrogen adsorption with a corresponding energy of −1.71 eV/N. In the case of atomic nitrogen absorption in the first subsurface layer of the $V_{75}Ru_{25}$/V(110) surface, the nitrogen atom still prefers to reside in the O-site. There are two unique O-sites in the first subsurface layer. One of these is coordinated with the Ru atom on the surface as shown in the O-site of Figure 13a. The other O-site

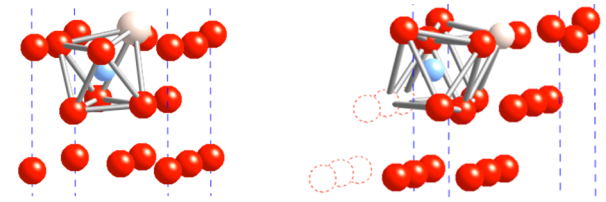

(a) O-site, E_{abs} = -0.48 eV/N **(b) O′-site, E_{abs} = -1.42 eV/N**

Figure 13. Optimized structure of atomic nitrogen at the first subsurface O-sites of the $V_{75}Ru_{25}$/V(110) surface: (a) O-site and (b) O′-site.

as illustrated in Figure 13b is only associated with the V atoms and is termed the O′-site. The absorption energies of atomic nitrogen at both O-sites are included in Figure 13. It is clear that the O′-site has the stronger adsorption energy of the two. The comparison between the adsorption energy on the surface and in the subsurface indicates that both subsurface sites are thermodynamically unfavorable and an activation barrier is involved for the subsurface diffusion process. Calculations based on the CI-NEB approach will be performed in future work to determine the barrier associated with the subsurface diffusion of the nitrogen atom into the $V_{75}Ru_{25}$/V(110) surface in addition to other V−Ru compositions and V-based alloy systems.

To understand the effect of alloying on the adsorption strength, it is important to realize the consequence upon alloying V with Ru. One interesting result is the change in the electronic structure, i.e., the d-band center. The electronic properties of the alloy are altered from the original properties of

dx.doi.org/10.1021/jp411763k | J. Phys. Chem. C 2014, 118, 4238−4249

the pure metal surface, and they affect the strength of the adsorption. By changing the location of the d-band center via alloying, the adsorption energy of atomic nitrogen on metal surfaces can be strengthened or weakened. The d-band center is the centroid of the d-orbital density of states and is calculated by taking the first moment of the projected density of states up to the Fermi level.[58] As the d-band center moves closer to the Fermi level, the bond between the adsorbate and the metal surface becomes stronger since more antibonding states exist above the Fermi level, and these states are empty. The opposite trend is observed when the d-band center is shifted down (further from the Fermi level) and the antibonding states become filled so that the bond between the metal surface and the adsorbate is weakened.[36]

Table 6 lists the d-band center for the surface metal atom of the bare V(110) and the $V_{75}Ru_{25}$/V(110) surfaces. To

Table 6. Surface d-Band Centers of Bare V(110) and $V_{75}Ru_{25}$/V(110) Surfaces

	ε_d (eV)	V_{ad}^2 [61,62]	$\varepsilon_{d,weighted}$ (eV)
	V(110)		
V (top layer)	−1.20	3.15	−1.20
	$V_{75}Ru_{25}$/V(110)		
V (top layer)	−1.50	3.15	−1.82
Ru	−2.61	3.87	

appropriately take into account the differences in the interaction of V and Ru with nitrogen, the weighted d-band center must be employed to represent the electronic structure of the surface. This concept was first introduced in the analysis of hydrogen chemisorption on Pd−Re alloyed overlayers and surfaces.[59] The weighted d-band center for a given surface can be calculated from eq 3

$$\varepsilon_{d,weighted} = \frac{V_{Ru}^2 \varepsilon_d^{Ru} N_{Ru} + V_V^2 \varepsilon_d^V N_V}{V_{Ru}^2 N_{Ru} + V_V^2 N_V} \quad (3)$$

where $\varepsilon_{d,weighted}$ is the weighted d-band center for the surface using the d-band center model,[60] V^2 is the d-band coupling matrix element for the surface metal atom, and N_{Ru} and N_V are the number of Ru−N and V−N bonds formed by the chemisorbed N atom, respectively. Considering the atomic nitrogen adsorption at the LB site of the alloy surface, the number of Ru−N and V−N bonds at this particular site is 3 and 1, respectively. From Table 6, alloying the V(110) surface with Ru affects the weighted d-band center of the surface by downshifting the weighted d-band center away from the Fermi level, compared to the weighted d-band center of the pure V(110) surface. Consequently, the interaction of atomic nitrogen with the surface metal layer becomes weaker on the $V_{75}Ru_{25}$/V(110) surface as presented earlier.

To summarize, alloying Ru with the V(110) surface apparently destabilizes the adsorption of the nitrogen atom on the surface and in the first subsurface layer. By introducing different metals to the surface, the electronic property, i.e., the d-band center of the surface, is modified, thereby affecting the reactivity of the surface.

4. CONCLUSIONS

It is well-known that group V metals have strong-binding characteristics to diatomic molecules such as N_2, O_2, H_2, and CO. These metals are of interest to investigate for small molecule reactivity to the extent of potential atomic diffusion into their bulk crystal structures. Fundamental study for molecular adsorption, dissociation of N_2, and potential subsequent atomic diffusion within the V(110) surface and V/Ru alloys has been investigated.

Electronic structure calculations based on DFT have been carried out to investigate molecular N_2 and the atomic nitrogen adsorption. At a 0.25 ML surface coverage, the results from the adsorption of molecular N_2 indicate three stable adsorbed N_2 states on the V(110) surface, i.e., weakly bounded γ-N_2 and strongly bounded α-N_2 and α'-N_2 states. These states are equivalent to the γ-N_2, α-N_2, and α'-N_2 states on the Fe(111) surface, respectively. The α- and α'-N_2 states are anticipated to be the most likely initial state for N_2 dissociation on the V(110) surface because the N_2 molecule is most elongated and the N−N stretching vibrational frequency is small, indicating a weak N−N bond. Similar to the adsorption of molecular N_2, the nitrogen atom also prefers the high coordination site.

The adsorption energies of the N_2 molecule and the nitrogen atom at the most stable site on the V(110) surface are considerably stronger than those on Fe and Ru surfaces because the location of the d-band center of V is higher in energy, compared to the d-band center of Fe or Ru. The N_2 dissociation path and its corresponding dissociation barrier are determined by applying the CI-NEB method. The following path is proposed: γ-N_2 → α'-N_2 → β-N, with a dissociation barrier of 0.4 eV. This barrier is comparable to the dissociation barrier at the Ru(0001) step. Since Ru is a common catalyst for ammonia synthesis, which involves N_2 dissociation, it can be concluded that the V(110) surface may be an active surface for N_2 dissociation. In addition to the dissociation barrier of N_2 on the V(110) surface, the barrier for the subsurface diffusion is also an important parameter to determine the feasibility of nitrogen transport through a metallic membrane. The subsurface octahedral (O-) site was found to be the most stable location for atomic nitrogen to reside in the V(110) subsurface layers. The energy change from atomic nitrogen on the surface to atomic nitrogen in the first subsurface layer is slightly endothermic. The corresponding subsurface diffusion barrier is 1.39 eV. Compared to the N_2 dissociation barrier on the V(110) surface, it can be concluded that the first subsurface diffusion step is the rate-limiting step for nitrogen transport across the metallic membrane.

To determine the feasibility of using pure vanadium as a material for a N_2-selective membrane, the first subsurface diffusion barrier of the N/V system is compared with the well-studied H/Pd case. The barrier for the first diffusion step for the N/V(110) surface is obviously larger than that for the H/Pd system. Therefore, it is possible that the nitrogen atom is likely to stay on the V(110) surface instead of diffusing into the subsurface layer. This surface stability of nitrogen is undesirable for the N_2-selective membrane application. Alloying V with Ru appears to alter the electronic structure of the surface and affect the adsorption energy of the nitrogen atom. To investigate the effect of alloying, one surface V atom was replaced by an atomic Ru to represent the $V_{75}R_{25}$/V(110) surface, which maintains the bcc crystal structure of the alloy at high temperature (700−800 °C). Alloying Ru with the V(110) surface apparently destabilizes the adsorption of the nitrogen atom on the surface and in the first subsurface layer. By introducing different metals to the surface, the d-band center of the surface may be modified, thereby affecting the surface reactivity.

dx.doi.org/10.1021/jp411763k | J. Phys. Chem. C 2014, 118, 4238−4249

In conclusion, pure vanadium may not be the best material option for the N_2-selective membrane because of its strong adsorption energy of atomic nitrogen and the high barrier for the first diffusion step into the subsurface. As a result, nitrogen transport through a pure V surface may be difficult to achieve. However, alloying V with Ru weakens the adsorption of nitrogen on the surface and in the first subsurface layer, which ultimately may decrease the barrier of the first step in subsurface diffusion. Future direction for this research using theoretical modeling from first-principles should include further consideration of other V−Ru alloy compositions that may provide optimal catalytic properties for N_2 dissociation and subsequent diffusion into the surface. In addition, the feasibility of ammonia synthesis on the V−Ru alloy should also be considered.

■ ASSOCIATED CONTENT

Ⓢ Supporting Information

All the geometry optimizations, adsorption energies, and bulk diffusion barrier calculations. This material is available free of charge via the Internet at http://pubs.acs.org.

■ AUTHOR INFORMATION

Corresponding Author

*E-mail jen.wilcox@stanford.edu; Tel (650) 724-9449; Fax (650) 725-2099 (J.W.).

Notes

The authors declare no competing financial interest.

■ ACKNOWLEDGMENTS

We acknowledge the high performance computing (HPC) facilities in the Center for Computational Earth and Environmental Science (CEES) at Stanford University, and the Texas Advanced Computing Center (TACC), at the University of Texas at Austin for providing HPC resources that have contributed to the research results reported within this paper.

■ REFERENCES

(1) Lu, G. Q.; Diniz da Costa, J. C.; Duke, M.; Giessler, S.; Socolow, R.; Williams, R. H.; Kreutz, T. Inorganic Membranes for Hydrogen Production and Purification: A Critical Review and Perspective. *J. Colloid Interface Sci.* **2007**, *314* (2), 589−603.

(2) Phair, J. W.; Donelson, R. Developments and Design of Novel (Non-Palladium-Based) Metal Membranes for Hydrogen Separation. *Ind. Eng. Chem. Res.* **2006**, *45* (16), 5657−5674.

(3) Buxbaum, R. E.; Kinney, A. B. Hydrogen Transport through Tubular Membranes of Palladium-Coated Tantalum and Niobium. *Ind. Eng. Chem. Res.* **1996**, *35* (2), 530−537.

(4) Wipf, H. Solubility and Diffusion of Hydrogen in Pure Metals and Alloys. *Phys. Scr.* **2001**, *2001* (T94), 43−51.

(5) Steward, S. A. *Review of Hydrogen Isotope Permeability Through Materials*; UCRL-53441; Lawrence Livermore National Laboratory; National Technical Information Service, U.S. Department of Commerce: Springfield, VA, 1983.

(6) Jaffe, R.; Price, J.; Hitzman, M.; Slakey, F. Energy Critical Elements; http://www.aps.org/units/fps/newsletters/201107/jaffe.cfm.

(7) Koller, R.; Bergermayer, W.; Kresse, G.; Hebenstreit, E. L. D.; Konvicka, C.; Schmid, M.; Podloucky, R.; Varga, P. The Structure of the Oxygen Induced (1 × 5) Reconstruction of V(100). *Surf. Sci.* **2001**, *480* (1−2), 11−24.

(8) Davies, P. W.; Lambert, R. M. Another Unique Reconstruction of the V(100) Surface: p(2 × 2) Microfacets on a (111) Oriented Crystal. *Chem. Phys. Lett.* **1981**, *83* (3), 480−482.

(9) Nakayama, K.; Usami, S. LEED and EELS Studies on Vanadium (110) and (111) Single Crystal Surfaces. *Surf. Sci.* **1993**, *287−288* (Part 1), 355−360.

(10) Nakayama, K.; Sato, T.; Usami, S.; Iwatsuki, M. Low-Energy Electron Diffraction and Scanning Tunneling Microscopy Study on the Reconstruction of the Vanadium (111) Surface. *Jpn. J. Appl. Phys.* **1995**, *34*, 589−594.

(11) Beutl, M.; Lesnik, J.; Lundgren, E.; Konvicka, C.; Varga, P.; Rendulic, K. D. Interaction of H_2, CO and O_2 with a Vanadium (111) Surface. *Surf. Sci.* **2000**, *447* (1−3), 245−258.

(12) Eibl, C.; Winkler, A. Time-of-Flight Studies on Desorbing and on Scattered D_2 Molecules from a V(111) + S Surface. *Surf. Sci.* **2001**, *482−485*, 201−206.

(13) Eibl, C.; Winkler, A. Angular and Energy Distributions of D_2 Molecules Desorbing from Sulfur and Oxygen Modified V(111) Surfaces. *J. Chem. Phys.* **2002**, *117* (2), 834−841.

(14) Kresse, G.; Hafner, J. Ab Initio Molecular Dynamics for Open-Shell Transition Metals. *Phys. Rev. B* **1993**, *48* (17), 13115−13118.

(15) Kresse, G.; Furthmüller, J. Efficiency of Ab-initio Total Energy Calculations for Metals and Semiconductors Using a Plane-Wave Basis Set. *Comput. Mater. Sci.* **1996**, *6* (1), 15−50.

(16) Blöchl, P. E. Projector Augmented-Wave Method. *Phys. Rev. B* **1994**, *50* (24), 17953−17979.

(17) Kresse, G.; Furthmüller, J. Efficient Iterative Schemes for Ab Initio Total-Energy Calculations Using a Plane-Wave Basis Set. *Phys. Rev. B: Condens. Matter* **1996**, *54* (16), 11169−11186.

(18) Perdew, J. P.; Burke, K.; Ernzerhof, M. Generalized Gradient Approximation Made Simple. *Phys. Rev. Lett.* **1996**, *77* (18), 3865.

(19) Monkhorst, H. J.; Pack, J. D. Special Points for Brillouin-Zone Integrations. *Phys. Rev. B* **1976**, *13* (12), 5188−5192.

(20) Methfessel, M.; Paxton, A. T. High-Precision Sampling for Brillouin-Zone Integration in Metals. *Phys. Rev. B* **1989**, *40* (6), 3616−3621.

(21) Henkelman, G.; Uberuaga, B. P.; Jónsson, H. A Climbing Image Nudged Elastic Band Method for Finding Saddle Points and Minimum Energy Paths. *J. Chem. Phys.* **2000**, *113* (22), 9901−9904.

(22) *CRC Handbook of Chemistry and Physics*, 92nd ed.; Haynes, W. M., Ed.; CRC Press/Taylor and Francis: Boca Raton, FL, Internet Version, 2012.

(23) Rao, C. N. R.; Ranga Rao, G. Nature of Nitrogen Adsorbed on Transition Metal Surfaces as Revealed by Electron Spectroscopy and Cognate Techniques. *Surf. Sci. Rep.* **1991**, *13* (7), 223−263.

(24) Mortensen, J. J.; Hansen, L. B.; Hammer, B.; Nørskov, J. K. Nitrogen Adsorption and Dissociation on Fe(111). *J. Catal.* **1999**, *182* (2), 479−488.

(25) Grunze, M.; Strasser, G.; Golze, M. Precursor Mediated and Direct Adsorption of Molecular Nitrogen on Fe{111}. *Appl. Phys. A: Mater. Sci. Process.* **1987**, *44* (1), 19−29.

(26) Bozso, F.; Ertl, G.; Grunze, M.; Weiss, M. Interaction of Nitrogen with Iron Surfaces: I. Fe(100) and Fe(111). *J. Catal.* **1977**, *49* (1), 18−41.

(27) Ertl, G.; Lee, S. B.; Weiss, M. Kinetics of Nitrogen Adsorption on Fe(111). *Surf. Sci.* **1982**, *114* (2−3), 515−526.

(28) Mortensen, J. J.; Morikawa, Y.; Hammer, B.; Nørskov, J. K. A Comparison of N_2 and CO Adsorption on Ru(001). *Z. Phys. Chem.* **1997**, *198* (1−2), 113−122.

(29) Anton, A. B.; Avery, N. R.; Toby, B. H.; Weinberg, W. H. The Chemisorption of Nitrogen on the (001) Surface of Ruthenium. *J. Electron Spectrosc. Relat. Phenom.* **1983**, *29* (1), 181−186.

(30) Spencer, N. D.; Schoonmaker, R. C.; Somorjai, G. A. Iron Single Crystals as Ammonia Synthesis Catalysts: Effect of Surface Structure on Catalyst Activity. *J. Catal.* **1982**, *74* (1), 129−135.

(31) Strongin, D. R.; Bare, S. R.; Somorjai, G. A. The Effects of Aluminum Oxide in Restructuring Iron Single Crystal Surfaces for Ammonia Synthesis. *J. Catal.* **1987**, *103* (2), 289−301.

(32) Dumesic, J. A.; Topsøe, H.; Boudart, M. Surface, Catalytic and Magnetic Properties of Small Iron Particles: III. Nitrogen Induced Surface Reconstruction. *J. Catal.* **1975**, *37* (3), 513−522.

(33) Boudart, M.; Loffler, D. G. Surface-Structure of Iron Catalysts for Ammonia-Synthesis. *J. Phys. Chem.* **1984**, *88* (23), 5763−5763.
(34) Strongin, D. R.; Carrazza, J.; Bare, S. R.; Somorjai, G. A. The Importance of C7 Sites and Surface Roughness in the Ammonia Synthesis Reaction over Iron. *J. Catal.* **1987**, *103* (1), 213−215.
(35) Fromm, E.; Mayer, O. Interaction of Oxygen and Nitrogen with Clean Transition Metal Surfaces. *Surf. Sci.* **1978**, *74* (1), 259−275.
(36) Hammer, B.; Nørskov, J. K.; Bruce, C.; Gates, H. K. Theoretical Surface Science and Catalysis—Calculations and Concepts. *Adv. Catal.* **2000**, *45*, 71−129.
(37) Bligaard, T.; Nørskov, J. K. In *Chemical Bonding at Surfaces and Interfaces*, 1st ed.; Nilsson, A., Pettersson, L. G. M., Nørskov, J. K., Eds.; Elsevier: Amsterdam, 2008; Chapter 4.
(38) Bozso, F.; Ertl, G.; Weiss, M. Interaction of Nitrogen with Iron Surfaces: II. Fe(110). *J. Catal.* **1977**, *50* (3), 519−529.
(39) Scholten, J. J. F.; Zwietering, P.; Konvalinka, J. A.; de Boer, J. H. Chemisorption of Nitrogen on Iron Catalysts in Connection with Ammonia Synthesis. Part 1. The Kinetics of the Adsorption and Desorption of Nitrogen. *Trans. Faraday Soc.* **1959**, *55*, 2166−2179.
(40) Imbihl, R.; Behm, R. J.; Ertl, G.; Moritz, W. The Structure of Atomic Nitrogen Adsorbed on Fe(100). *Surf. Sci.* **1982**, *123* (1), 129−140.
(41) Mortensen, J. J.; Ganduglia-Pirovano, M. V.; Hansen, L. B.; Hammer, B.; Stoltze, P.; Nørskov, J. K. Nitrogen Adsorption on Fe(111), (100), and (110) Surfaces. *Surf. Sci.* **1999**, *422* (1−3), 8−16.
(42) Tománek, D.; Bennemann, K. H. Total-Energy Calculations for N_2 Dissociation on Fe(111): Characterization of Precursor and Dissociative States. *Phys. Rev. B* **1985**, *31* (4), 2488−2490.
(43) Grunze, M.; Strasser, G.; Golze, M.; Hirschwald, W. Thermodynamic and Kinetic Parameters of Molecular Nitrogen Adsorption on Fe{111}. *J. Vac. Sci. Technol., A* **1987**, *5* (4), 527−534.
(44) Hummelshøj, J. S.; Abild-Pedersen, F.; Studt, F.; Bligaard, T.; Nørskov, J. K. CatApp: A Web Application for Surface Chemistry and Heterogeneous Catalysis. *Angew. Chem., Int. Ed.* **2012**, *51* (1), 272−274.
(45) Logadóttir, Á.; Nørskov, J. K. Ammonia Synthesis over a Ru(0001) Surface Studied by Density Functional Calculations. *J. Catal.* **2003**, *220* (2), 273−279.
(46) Honkala, K.; Hellman, A.; Remediakis, I. N.; Logadottir, A.; Carlsson, A.; Dahl, S.; Christensen, C. H.; Nørskov, J. K. Ammonia Synthesis from First-Principles Calculations. *Science* **2005**, *307* (5709), 555−558.
(47) Ozdogan, E. Theoretical and Experimental Investigations of Metallic Membranes for CO_2 Capture. Ph.D. Dissertation, Stanford University, Stanford, CA, 2012.
(48) Jiang, D. E.; Carter, E. A. Carbon Dissolution and Diffusion in Ferrite and Austenite from First Principles. *Phys. Rev. B* **2003**, *67* (21), 214103−1−11.
(49) Jiang, D. E.; Carter, E. A. Carbon Atom Adsorption on and Diffusion into Fe(110) and Fe(100) from First Principles. *Phys. Rev. B* **2005**, *71* (4), 045402−1−6.
(50) Paglieri, S. N.; Way, J. D. Innovations in Palladium Membrane Research. *Sep. Purif. Rev.* **2002**, *31* (1), 1−169.
(51) Ferrin, P.; Kandoi, S.; Nilekar, A. U.; Mavrikakis, M. Hydrogen Adsorption, Absorption and Diffusion on and in Transition Metal Surfaces: A DFT Study. *Surf. Sci.* **2012**, *606* (7−8), 679−689.
(52) Dolan, M. D. Non-Pd BCC Alloy Membranes for Industrial Hydrogen Separation. *J. Membr. Sci.* **2010**, *362* (1−2), 12−28.
(53) Wu, M. H.; Liu, X. H.; Gu, J. F.; Jin, Z. H. First-Principles Simulations of Iron with Nitrogen: From Surface Adsorption to Bulk Diffusion. *Modell. Simul. Mater. Sci. Eng.* **2013**, *21* (4), 045004−1−14.
(54) Jiang, D. E.; Carter, E. A. Adsorption and Diffusion Energetics of Hydrogen Atoms on Fe(110) from First Principles. *Surf. Sci.* **2003**, *547* (1−2), 85−98.
(55) Paglieri, S. N. Palladium Membranes. In *Nonporous Inorganic Membranes*; Wiley-VCH Verlag GmbH & Co. KGaA: Weinheim, 2006; pp 77−105.
(56) Dahl, S.; Logadottir, A.; Jacobsen, C. J. H.; Nørskov, J. K. Electronic Factors in Catalysis: The Volcano Curve and the Effect of Promotion in Catalytic Ammonia Synthesis. *Appl. Catal., A* **2001**, *222* (1−2), 19−29.
(57) Smith, J. F. *Ru-V (Ruthenium-Vanadium) Phase Diagram*; ASM International: Materials Park, OH, 1990.
(58) Hammer, B.; Nielsen, O. H.; Nørskov, J. K. Structure Sensitivity in Adsorption: CO Interaction with Stepped and Reconstructed Pt Surfaces. *Catal. Lett.* **1997**, *46* (1−2), 31−35.
(59) Pallassana, V.; Neurock, M.; Hansen, L. B.; Norskov, J. K. First Principles Analysis of Hydrogen Chemisorption on Pd-Re Alloyed Overlayers and Alloyed Surfaces. *J. Chem. Phys.* **2000**, *112* (12), 5435−5439.
(60) Hammer, B.; Nørskov, J. K. Electronic Factors Determining the Reactivity of Metal Surfaces. *Surf. Sci.* **1995**, *343* (3), 211−220.
(61) Greeley, J.; Norskov, J. K.; Mavrikakis, M. Electronic Structure and Catalysis on Metal Surfaces. *Annu. Rev. Phys. Chem.* **2002**, *53*, 319−348.
(62) Ruban, A.; Hammer, B.; Stoltze, P.; Skriver, H. L.; Nørskov, J. K. Surface Electronic Structure and Reactivity of Transition and Noble Metals. *J. Mol. Catal. A: Chem.* **1997**, *115* (3), 421−429.